Available online at www.sciencedirect.com

ScienceDirect

Procedia Structural Integrity 41 (2022) 461–469

Structural Integrity Procedia

www.elsevier.com/locate/procedia

2nd Mediterranean Conference on Fracture and Structural Integrity

Root rotations and root displacements in bimaterial layers and thin films

Roberta Massabò[a]*, Konstantin Ustinov[b]

[a] *Department of Civil, Chemical and Environmental Engineering, University of Genova, Via Montallegro 1, Genova 16145, Italy*
[b] *Laboratory of Geomechanics, A. Yu. Ishlinsky Institute for Problems in Mechanics, RAS, Moscow 119526, Russia*

Abstract

An elasticity technique to derive compliance coefficients describing crack tip root rotations and displacements in end-loaded, bimaterial, isotropic and orthotropic layers has been recently proposed in Ustinov and Massabò (Int. J. Solids Struct., 2022). The coefficients define the boundary conditions which account for the near tip deformations when using beam (plate) theories to describe the detached layers. The coefficients, collected into 6x6 compliance matrices, relate crack tip kinematic variables describing relative displacements and rotations between the detached and intact parts, and six elementary crack tip loadings, which combine to describe general end loadings. The steps necessary to use the coefficients in the solution of statically determined problems, when the forces acting on the layer are known through equilibrium, is presented here with reference to classical fracture mechanics specimens.

Keywords: Delamination; Bimaterial layers; Elastic clamping; Reciprocity theorem

1. Introduction

Beam and plate theories are extensively used to analyze layered structures and specimens with delaminations. They are applied to study classical laminates, composite sandwich beams, layered systems and thin films on thick substrates as well as for novel materials and systems used in soft electronics, biomaterial applications or in coatings (e.g., Kanninen (1973); Bao et al. (1992); Thouless (2018); Massabò (2022,2014); Monetto and Massabò (2020); Massabò

* Corresponding author. Tel.: +39-010-335-2956; fax: +39-010-335-1546.
E-mail address: Roberta.massabo@unige.it

10.1016/j.prostr.2022.05.052

and Darban (2019). In many cases they provide results which are exact or very closed to the exact results (Ciarlet, 1997). When using these theories to analyze detached layers, the boundary conditions at the crack tip cross sections typically differ from the built-in condition, which may be used only for special configurations, such as layers with very long cracks, due to the presence of non-negligible near tip deformations in general cases. Proper boundary conditions must reproduce the actual imperfect elastic clamping conditions, and this is typically done through the introduction of root rotations and root displacements (see for instance Cotterell and Chen (2000); Yu and Hutchinson (2002); Monetto and Massabò (2020).

Recently, Ustinov and Massabò (2022) have presented a 2-D elasticity technique based on the use of exact fields far away from the crack tip, the J-integral and the reciprocity theorem to define relations between the compliance coefficients describing root rotations and displacements and the J-integral terms associated to six elementary loadings. The relations allow to define most of the compliance coefficients from analytical or numerical results for the energy release rate. In addition, for special problems, which include bimaterial isotropic layers with mid-thickness cracks and zero second Dundur's parameter, homogeneous symmetric orthotropic layers and thin films on half-planes, explicit expressions have been derived for the coefficients. In combination with previous results obtained in Ustinov (2015), Ustinov (2019), Ustinov et al. (2020), Massabò et al. (2019), these solutions provide full analytical description of problems characterized by extreme elastic properties, both in isotropic and orthotropic systems. They are therefore valuable for current applications, for instance in soft electronics, Begley and Hutchinson (2017).

In this paper, the steps necessary to use the compliance coefficients associated to the elementary loadings to describe root rotation and root displacements and displacement fields in fracture specimens, where the applied forces are known from equilibrium, are presented. Reference is made to classical fracture mechanics tests: the Double Cantilever Beam specimen, both homogeneous and asymmetric, and the End Loaded Split specimen. The solutions are compared with finite element results from the literature.

2. Problem and matrix of elastic compliances

The 2-D problem of a bimaterial layer with a through thickness interfacial crack, shown in Fig. 1, is considered. The lower and upper parts of the layer have thicknesses h_1 and h_2, with $\eta = h_1 / h_2$ and the materials are linearly elastic, isotropic or orthotropic with principal material axes parallel to the boundaries. The layer is subjected to arbitrary end loadings applied at distances l_1, l_2, l_3 from the crack tip; the distances are such to ensure that the effects of the loadings on the crack tip can be described by end force and moment resultants and that the crack tip stresses do not affect the end sections. The applied loadings generate axial and shear forces, P_i, V_i, and bending moments, M_i, with $i = 1, 2, 3$, at the crack tip cross sections.

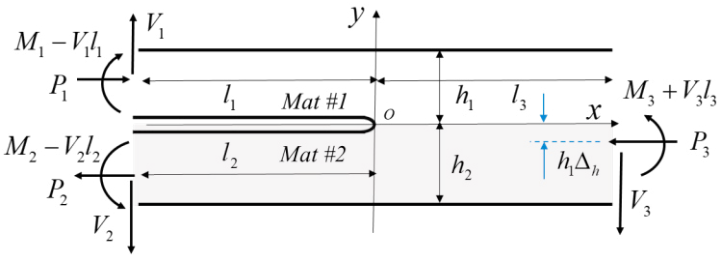

Fig. 1. Bimaterial isotropic/orthotropic layer with interfacial crack subject to end loadings

The statics of the layer is described by six elementary crack tip loadings (e.g., Suo and Hutchinson (1990); Li et al, (2004), Ustinov (2015,2019), Andrews and Massabò (2007), Massabò et al. (2019)). Figure 2 shows the elementary loadings which are most used in the literature. Four of them produce crack tip singularity and are:

1) axial forces with compensating bending moment applied at the lower arm:

$$P_S = P_1 - \Sigma\left(\Sigma + \eta^{-1}\right)^{-1} P_3 - \Sigma(\Delta_h + 1/2) I^{-1} h_1^{-1} M_3 \tag{1}$$

2) symmetrical bending moments: $M_S = M_1 - \Sigma 12^{-1} I^{-1} M_3$ (2)

3) symmetrical shear forces (double shear): $D = V_2$ (3)

4) asymmetrical shear forces (single shear): $S = V_3$ (4)

where:

$$\Delta_h = \frac{1}{2\eta}\frac{1-\Sigma\eta^2}{1+\Sigma\eta}, \qquad I = \Sigma\left(\Delta_h^2 + \Delta_h + \frac{1}{3}\right) + \frac{\Delta_h^2}{\eta} - \frac{\Delta_h}{\eta^2} + \frac{1}{3\eta^3} \tag{5}$$

The elastic mismatch $\Sigma = \beta_{11(2)} / \beta_{11(1)}$, with $\beta_{11(i)}$ a constant of compliance in layer *i*, becomes $\Sigma = E_1 / E_2$ in isotropic layers under plane stress conditions, with E_i the Young's modulus in layer *i* and ν_i the Poisson coefficient. Extension to plane strain problems is straightforward.

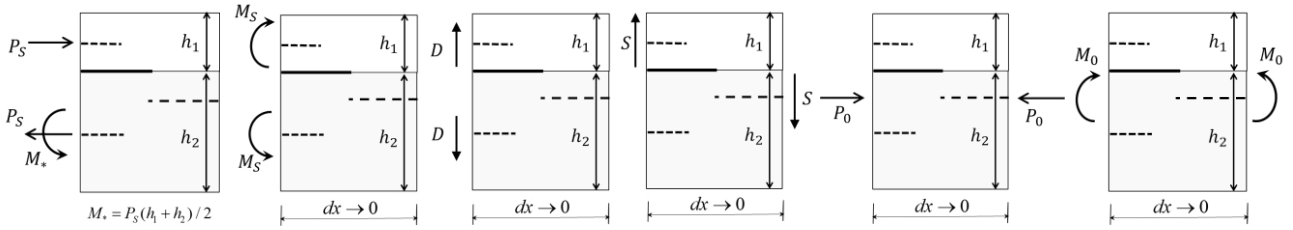

Fig. 2. Elementary loads 1-6 acting at the crack tip cross sections of the bimaterial layer

The last two elementary loadings, (5) and (6) in Fig. 2, are void loadings which do not produce singularity at the crack tip but affect the near tip deformations. The first void loading is uniform compression, with $P_0 = P_3$ so that $P_1 = P_0\Sigma\eta/(1+\Sigma\eta), P_2 = -P_0/(1+\Sigma\eta)$ for equilibrium. The second is uniform bending with $M_0 = M_3$ so that $M_1 = M_0\Sigma\eta^3(1+\Sigma\eta)/\chi$, $M_2 = -M_0(1+\Sigma\eta)/\chi, P_1 = P_2 = 6M_0h_1^{-1}\Sigma\eta^2(1+\eta)/\chi$ to satisfy equilibrium, with $\chi = \eta^4\Sigma^2 + 4\eta^3\Sigma + 6\eta^2\Sigma + 4\eta\Sigma + 1$.

The kinematics of the layer is described by longitudinal and transverse displacements, $u_{(i)}, v_{(i)}$ with $i = 1,2$ for the upper and lower sub-layers. Different kinematic variables have been used in Ustinov and Massabò (2022) to define the boundary conditions for the detached layers, when they are studied as beams or plates. The original derivation has been based on the relative displacements and rotations of the neutral lines of the detached layers and the interface. The solutions have then been modified to describe different kinematic variables. Here solutions are presented for the kinematic variables which are used in Timoshenko type beam theory. They are defined as: crack tip relative longitudinal displacements, $u_1 = u_{(1)}(x=0^-, y=h_1/2) - u_{(2)}(x=0^+, y=-h_1\Delta_h)$ and $u_2 = u_{(2)}(x=0^-, y=-h_2/2) - u_{(2)}(x=0^+, y=-h_1\Delta_h)$ and relative transverse displacements, v_1 and v_2 (having similar forms), between the neutral axes of the detached and intact parts of the layer (formulas presented for the case $h_1\Delta_h \geq 0$); and relative rotations, φ_1 and φ_2, of the cross sections between the two parts. They are shown in the schematic in Fig. 3.

The way to define the rotations is not unique. In Ustinov and Massabò (2022) the coefficients associated to the rotations of the cross sections have been defined so that the averaged squares of the difference between the real horizontal displacements and the displacements due to rotation by this angle over the layer thickness be minimal.

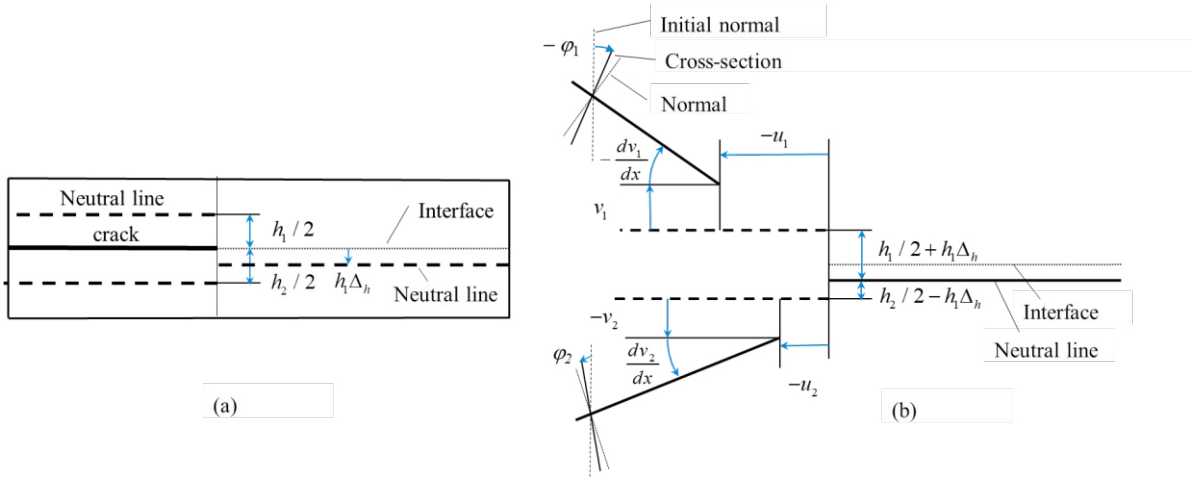

Fig. 3. (a) Bimaterial layer, undeformed configuration; (b) root rotations and root displacements defined as relative displacements between the neutral axes of the detached and intact parts (solid-thick lines: deformed configuration; dashed lines: undeformed configuration).

The matrix of compliances, which relate the kinematic variables to the elementary loadings is:

$$\begin{pmatrix} u_1 \\ -\varphi_1 h_1 \\ v_1 \\ u_2 \\ -\varphi_2 h_1 \\ v_2 \end{pmatrix} = \begin{pmatrix} a_{11} & a_{12} & a_{13} & a_{14} & 0 & 0 \\ a_{21} & a_{22} & a_{23} & a_{24} & 0 & 0 \\ a_{31} & a_{32} & a_{33} & a_{34} & a_{35} & a_{36} \\ a_{41} & a_{42} & a_{43} & a_{44} & 0 & 0 \\ a_{51} & a_{52} & a_{53} & a_{54} & 0 & 0 \\ a_{61} & a_{62} & a_{63} & a_{64} & a_{65} & a_{66} \end{pmatrix} \begin{pmatrix} P_S \\ M_S h_1^{-1} \\ D \\ S \\ P_0 \\ M_0 h_1^{-1} \end{pmatrix} \tag{6}$$

where the coefficients a_{ij} have been related in Ustinov and Massabò (2002) to the terms of the energy release rate associated to the elementary loads by using exact solutions for the displacement fields far away from the crack tip and the reciprocity theorem of 2-D elasticity. Explicit expressions for the coefficients have been obtained for: bimaterial isotropic layers with mid-thickness cracks (26 out of the 28 coefficients derived along with a relation for the last two, a_{34}, a_{64}); homogeneous orthotropic symmetric layers (all coefficients but $a_{33} = -a_{63}$ and $a_{34} = -a_{64}$); and relevant coefficients describing thin films on half-planes. For isotropic layers with second Dundurs' parameter $\beta = 0$, the coefficients depend on the first Dundur's parameter $\alpha = (\Sigma - 1)/(\Sigma + 1)$ and some analytic functions, $\delta, \delta_P, g_{33}, g_{34}$ given in Ustinov and Massabò (2022).

3. Application to fracture mechanics specimens with known crack tip forces

The compliance coefficients in the matrix in Eq. 6 can be used to calculate root rotations and root displacements in fracture specimens and layered structures. In this section some examples will be presented with reference to the specimens analyzed by Qiao and Wang (2004). The analytical results will then be compared with finite elements solutions from the same paper or obtained by Ustinov and Massabò (2022.)

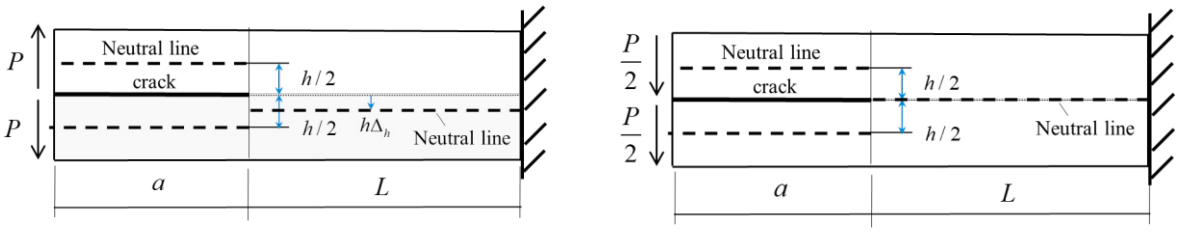

Fig. 4. (a) Double Cantilever Beam specimen (DCB)/Asymmetric Double Cantilever Beam specimen (ADCB). (b) End Loaded Split (ELS) specimen

3.1. Application to homogeneous DCB and asymmetric ADCB specimens

The first case examined is the Double Cantilever Beam specimen with equal ($\alpha=\beta=0$, DCB) and unequal isotropic layers ($\alpha\neq 0$, $\beta=0$ and $\beta\neq 0$, ADCB), of the same thickness $h_1=h_2=h$ ($\eta=1$) shown in Fig. 4. The applied loads are localized symmetric transverse forces P applied at the ends of the detached layers. In both cases $\chi=\Sigma^2+14\Sigma+1$ and $\Delta_h=(1-\Sigma)/(2+2\Sigma)=-\alpha/2$, which particularize to $\chi=16$, $\Delta_h=0$ and $I=2/3$ for the homogeneous symmetric DCB, where the neutral axis of the intact layer is at mid-thickness.

The applied loads generate crack tip force and moment resultants which are described by the elementary loads for symmetric bending, $M_S=Pa$, and double shear, $D=P$, while the other elementary loads vanish, $P_S=S=P_0=0, M_0=0$. Root rotations and root displacements for $\beta=0$, using Eq. 6, and the associated coefficients are listed below.

• Longitudinal root displacements in DCB/ADCB specimens:

$$u_1=P(a_{12}\frac{a}{h}+a_{13}),u_2=P(a_{42}\frac{a}{h}+a_{43}), \tag{7}$$

with $$a_{12}=-\frac{\sqrt{3}\alpha}{E_1\sqrt{4-3\alpha^2}},\ a_{13}=\frac{1}{E_1}\left(\frac{\alpha}{2}-\frac{\alpha\delta\sqrt{3}}{\sqrt{4-3\alpha^2}}+\frac{\nu_1}{2}\right),$$

$$a_{42}=-a_{12}\frac{1+\alpha}{1-\alpha},\ a_{43}=\frac{1}{E_1}\left[\frac{\sqrt{3}\alpha\delta}{\sqrt{4-3\alpha^2}}-\frac{\alpha}{2}+\frac{\nu_2}{2}\right]\frac{(1+\alpha)}{(1-\alpha)}$$

• Transverse root displacements in DCB/ADCB specimens:

$$v_1=P(a_{32}\frac{a}{h}+a_{33}),v_2=P(a_{62}\frac{a}{h}+a_{63}), \tag{8}$$

with: $$a_{32}=\frac{1}{E_1}\left(-\frac{6}{5}+3\alpha+\frac{9\alpha^2}{2}+6\delta^2+\frac{6\sqrt{3}\alpha(1+\alpha)\delta_p}{\sqrt{4-3\alpha^2}}-\frac{3\nu_1}{2}\right),\ a_{33}=\frac{4+3\alpha}{2E_1(4-3\alpha^2)}\mathrm{g}_{33}-\frac{3(1+\alpha)}{E_1(4-3\alpha^2)}\mathrm{g}_{34}$$

$$a_{62}=\frac{3(1+\alpha)(4+10\alpha-15\alpha^2-20\delta^2)}{10E_1(1-\alpha)}+\frac{6\sqrt{3}\alpha(1+\alpha)\delta_p}{E_1\sqrt{4-3\alpha^2}}+\frac{3(1+\alpha)\nu_2}{2E_1(1-\alpha)},$$

$$a_{63} = -\frac{(1+\alpha)(4-3\alpha)}{2E_1(1-\alpha)(4-3\alpha^2)}\mathrm{g}_{33} - \frac{3(1+\alpha)}{E_1(4-3\alpha^2)}\mathrm{g}_{34}$$

• Root rotations in DCB/ADCB specimens:

$$\varphi_1 = -\frac{P}{h}(a_{22}\frac{a}{h} + a_{23}), \varphi_2 = -\frac{P}{h}(a_{52}\frac{a}{h} + a_{53}), \tag{9}$$

with: $$a_{22} = \frac{6\sqrt{3}\alpha(1+\alpha)}{E_1\sqrt{4-3\alpha^2}} + \frac{12\delta}{E_1}, a_{23} = \frac{1}{E_1}\left(\frac{6\sqrt{3}\alpha(1+\alpha)\delta}{\sqrt{4-3\alpha^2}} + 6\delta^2 - 3\alpha - \frac{3\alpha^2}{2} - \frac{6}{5}(1+\nu_1)\right)$$

$$a_{52} = \frac{6\sqrt{3}\alpha(1+\alpha)}{E_1\sqrt{4-3\alpha^2}} - \frac{12\delta}{E_1}\frac{1+\alpha}{1-\alpha}, a_{53} = \frac{1}{E_1}\left(\frac{6\sqrt{3}\alpha(1+\alpha)\delta}{\sqrt{4-3\alpha^2}} - \frac{(1+\alpha)}{(1-\alpha)}\left(6\delta^2 + 3\alpha - \frac{3\alpha^2}{2}\right) + \frac{6}{5}(1+\nu_2)\right)$$

For the homogeneous DCB specimen, the analytic functions assume values $\delta = 0.673$, $\delta_P = 0.209$, $g_{33} = 2.271$ and $g_{34} = 0$, and the compliance coefficients simplify yielding:

$$\begin{aligned} u_1 &= u_2 = \frac{\nu}{2E}P \\ v_1 &= -v_2 = \frac{6Pa}{Eh}\left(-\frac{1}{5} + 0.673^2 - \frac{\nu}{4}\right) + 2.271\frac{P}{2E} \\ \varphi_1 &= -\varphi_2 = -\frac{12P}{Eh}\left(0.673\frac{a}{h} - \frac{1}{10} + \frac{0.673^2}{2} - \frac{\nu}{10}\right) \end{aligned} \tag{10}$$

The calculated root rotations and displacements may be used as boundary conditions to accurately define displacements in the detached layers when using beam or plate theories. In accordance to Timoshenko beam theory, for instance, the load-point displacement in the homogeneous DCB may be obtained by superposing the contributions due to the flexural deflection of a built-in beam, the deflection due to shear deformations along the detached layer and the effects due to root rotation and root displacement at the crack tip given above. This yields:

$$v_{(1)}(x=-a) - v_{(2)}(x=-a) = 2\left(\frac{4Pa^3}{Eh^3} + \frac{12Pa}{5Eh}(1+\nu) - \varphi_1 a + v_1\right) \tag{11}$$

Comparing this result with the exact 2-D elasticity result in Ustinov and Massabò (2020) shows that the displacement in (11) is missing the term $\frac{3Pa}{5Eh}\nu$, which is due to shear deformations near the crack tip which are not included in the second term in the brackets.

The rotations of the neutral lines could be used instead of the rotations of the cross sections as kinematics variables to define the compliance matrix. This has been done in Ustinov and Massabò (2020) and the compliance matrix associated to this choice is provided in the paper. Using the compliance coefficients associated to the rotations of the neutral axes in combination with Euler Bernoulli beam theory, which provides the flexural deflection of the detached arm, yields a solution which coincides with the 2-D result.

3.2. Application to homogeneous ELS specimen

In the homogeneous ELS specimen, shown in Fig. 4, with $h_1 = h_2 = h$ ($\eta = 1$) and $\alpha = \beta = 0$, the crack tip field is more complex and described, through equations (7-10), by the five elementary loadings: symmetric bending,

$M_S = -3/8Pa$, axial forces, $P_S = 3Pa/(4h)$, double shear $D = P/2$, single shear $S = -P$, uniform bending $M_0 = -Pa$, while the void loading $P_0 = 0$. Root rotation and displacements depend on the elastic constants and the analytic functions $\delta = 0.673$, $\delta_P = 0.209$, $g_{33} = 2.271$ and $g_{34} = 0$.

• Longitudinal root displacements in homogeneous isotropic ELS specimen:

$$u_1 = Pa(\frac{3}{4h}a_{11} - \frac{3}{8h}a_{12} + \frac{a_{13}}{2a} - \frac{a_{14}}{a}), u_2 = -u_1, \tag{12}$$

with: $a_{11} = \dfrac{\delta_P}{E}$, $a_{12} = 0$, $a_{13} = \dfrac{\nu}{2E}$, $a_{14} = -\dfrac{3}{5E} - \dfrac{3\delta_P{}^2}{8E} - \dfrac{3\nu}{8E}$

Simple substitution yields: $u_1 = -u_2 = \dfrac{P}{E}\left(\dfrac{3}{8}\delta_P{}^2 + \dfrac{3}{5} + \dfrac{3}{4}\delta_P\dfrac{a}{h} + \dfrac{5}{8}\nu\right)$

• Transverse root displacements in homogeneous isotropic ELS specimen:

$$v_1 = Pa(\frac{3}{4h}a_{31} - \frac{3}{8h}a_{32} + \frac{a_{33}}{2a} - \frac{a_{34}}{a} - \frac{a_{36}}{h}), v_2 = v_1, \tag{13}$$

with: $a_{31} = \dfrac{1}{E}\left(-\dfrac{3}{5} + 3\delta^2 - 3\delta_P{}^2 - \dfrac{\nu}{2}\right)$, $a_{32} = \dfrac{1}{E_1}\left(-\dfrac{6}{5} + 6\delta^2 - \dfrac{3\nu}{2}\right)$, $a_{33} = \dfrac{g_{33}}{2E}$, $a_{34} = \dfrac{a_{33}}{2}$, $a_{36} = \dfrac{3\nu}{16E}$

Simple substitution shows that $v_1 = v_2 = -\dfrac{9\delta_P{}^2}{4Eh}Pa$

• Root rotations in homogeneous isotropic ELS specimen:

$$\varphi_1 = -\frac{Pa}{h}(\frac{3}{4h}a_{21} - \frac{3}{8h}a_{22} + \frac{a_{23}}{2a} - \frac{a_{24}}{a}),\ \varphi_2 = \varphi_1 \tag{14}$$

with: $a_{21} = \dfrac{6(\delta - \delta_P)}{E_1}$, $a_{22} = \dfrac{12\delta}{E_1}$, $a_{23} = \dfrac{1}{E_1}\left(6\delta^2 - \dfrac{6}{5}(1+\nu)\right)$, $a_{24} = \dfrac{1}{E_1}\left(3\delta^2 + \dfrac{9}{4}\delta_P{}^2 - \dfrac{3}{5}(1+\nu)\right)$

Simple substitution shows that $\varphi_1 = \dfrac{9}{4}\dfrac{P}{Eh}\left(\delta_P{}^2 + \dfrac{2a}{h}\delta_P\right)$, $\varphi_2 = \varphi_1$

4. Comparison with 2-D finite element results

Root rotations and root displacements in Eqs. (7-14) are compared in Table 1 with the FE results in Qiao and Wang (2004) and in Ustinov and Massabò (2022) for specimens with: $a = 16h_1$ and $\eta = h_1/h_2 = 1$. The layers in the homogeneous DCB specimen have Poisson ratio $\nu = 0.3$. In the ADCB specimen, bimaterial layers with $\alpha = -0.667$ and $\beta = -0.23$ (plane stress; $E_2 = 5E_1, \nu_1 = \nu_2 = 0.3$) and $\alpha = -0.667$ and $\beta = 0$ (plane stress; $E_2 = 5E_1, \nu_1 = 0.995, \nu_2 = 0.975$) are examined to investigate the effects of the simplifying assumption $\beta = 0$, which is usually made to avoid near tip oscillating fields. The comparison highlights that the classical assumption $\beta = 0$ is indeed acceptable when calculating root rotation coefficients while may yield important under/over-estimations of the root displacement coefficients.

5. Conclusions

The steps required to define root rotations and root displacements in bimaterial layers subjected to arbitrary end loadings using compliance coefficients associated to six elementary loadings and recently derived through an elasticity technique have been presented with reference to two classical fracture mechanics specimens, the Double Cantilever

Beam and End Loaded Split specimens. The application shows that all six elementary loads, including two void loadings, are necessary to define the displacement field, as opposed to the four elementary loads which fully define the fracture parameters. The comparison with finite element results from the literature highlights the effects of the second Dundurs' parameter on root displacements.

TABLE 1. Root rotations and root displacements in homogeneous isotropic DCB (with $\nu = 0.3$), bimaterial isotropic ADCB with $\alpha = -0.667$ and $\beta = -0.23, 0$ and homogeneous isotropic ELS specimens; in all cases $\eta = h_1 / h_2 = 1$ and crack length $a = 16 h_1$. Exact and FE results for bimaterial ADCB with $\beta = 0$ obtained in Ustinov and Massabò (2020). FE results for other cases obtained in Qiao and Wang (2004). Plane stress conditions.

SPECIMEN	SOLUTIONS	$-\frac{\varphi_1 E_1 h_1}{P}$	$-\frac{\varphi_2 E_1 h_1}{P}$	$-\frac{(\varphi_1-\varphi_2) E_1 h_1}{P}$	$\frac{u_1 E_1}{P}$	$\frac{u_2 E_1}{P}$	$\frac{v_1 E_1}{P}$	$\frac{v_2 E_1}{P}$	$\frac{(v_1-v_2) E_1}{P}$
DCB	Exact	130.4	-130.4	260.8	0.15	0.15	18.2	-18.2	36.4
	FEM	131.4	-131.4	262.9	0	0	20.7	-20.7	41.4
ADCB $\alpha = -0.667$	$\beta = 0$ Exact	88.3	-42.8	131.1	11.97	-2.17	-21.2	-22.2	1
	$\beta = 0$ FEM	91.8	-45.9	137.7	12.1	-2.2	-22	-22.3	0.3
	$\beta = -0.23$ FEM	97	-41.3	138.3	7.88	-1.78	1.6	-18.9	20.5
ELS	Exact	-15.1	-15.1	0	3.31	-3.31	-1.57	-1.57	0
	FEM	-13.3	-13.3	0	2.5	-2.5	0	0	0

Acknowledgements

This work was partially supported by the U.S. Office of Naval Research, ONR Global, contract # N62909-21-1-2048 (RM) and the Ministry of Science and Higher Education within the framework of the Russian State Assignment under contract No. A AAA-A20-120011690133-1 (KU).

References

Andrews, M., Massabo, R., 2007. The effects of shear and near tip deformations on energy release rate and mode mixity of edge-cracked orthotropic layers. Eng. Fract. Mech. 74 (17), 2700–2720

Bao, G., Ho, S., Suo, Z., Fan, B., The role of material orthotropy in fracture specimens for composites, Int. J. Solids Struct. 29 (9) (1992) 1105-1116. doi:10.1016/0020-7683(92)90138-j

Barbieri L, Massabò R, Berggreen C. The effects of shear and near tip deformations on interface fracture of symmetric sandwich beams. (2018) Eng Fract Mech, 201:298–321.

Begley, M.R, Hutchinson, J.W. The Mechanics and Reliability of Films, Multilayers and Coatings. Cambridge University Press, (2017)

Ciarlet, P.G., Mathematical Elasticity, Vol. II : Theory of Plates, Series "Studies in Mathematics and its Applications", North-Holland, Amsterdam, 1997.

Cotterell, B., Chen Z., 2000. Buckling and cracking of thin film on compliant substrates under compression. International Journal of Fracture 104 (2), 169–179.

Kanninen, M.F., 1973. An augmented double cantilever beam model for studying crack propagation and arrest. Int J Fracture 9, 83-92.

Li, S., Wang, J., Thouless, M., 2004. The effects of shear on delamination in layered materials. J. Mech. Phys. Solid. 52 (1), 193–214.

Massabò, R. (2014). Influence of boundary conditions on the response of multilayered plates with cohesive interfaces and delaminations using a homogenized approach. Frattura Ed Integrita Strutturale, 8(29), 230-240. doi:10.3221/IGF-ESIS.29.20

Massabò, R., Upper and lower bounds for the parameters of one-dimensional theories for sandwich fracture specimens (2021) J. Appl. Mech., Trans. ASME, 88 (3), art. no. 031014.

Massabò, R.; Ustinov, K.; Barbieri, L.; Berggreen, C. Fracture Mechanics Solutions for Interfacial Cracks between Compressible Thin Layers and Substrates. Coatings 2019, 9, 152.

Massabò, R., & Darban, H. (2019). Mode II dominant fracture of layered composite beams and wide-plates: A homogenized structural approach. Engineering Fracture Mechanics, 213, 280-301. doi:10.1016/j.engfracmech.2019.03.002

Monetto, I., Massabò, R., An analytical solution for the inverted four-point bending test in orthotropic specimens, Engineering Fracture Mechanics (2020), doi: https://doi.org/10.1016/j.engfracmech.

Monetto, I., Massabò, R. An analytical beam model for the evaluation of crack tip root rotations and displacements in orthotropic specimens, (2020) Frattura ed Integrità Strutturale, 14 (53), 372-393, DOI: 10.3221/IGF-ESIS.53.29

Suo ZG, Hutchinson JW. Interface crack between two elastic layers. Int J Fract 1990;43:1–18

Thouless, M.D. Shear forces, root rotations, phase angles and delamination of layered materials. Eng. Fract. Mech. 2018, 191, 153–167
Qiao, P, and Wang, J, Mechanics and fracture of crack tip deformable bi-material interface, Int. J. Solids and Structures, 2004, 41, 7423-7444
Ustinov, K.B., Massabò, R., On elastic clamping boundary conditions in plate models describing detaching bilayers, Int. J. Solids Struct., 2022, in press
Ustinov KB., On separation of a layer from the half-plane: Elastic fixation conditions for a plate equivalent to the layer. (2015) Mech Solids;50: 62–80.
Ustinov, K.B., On semi-infinite interface crack in bi-material elastic layer, European J. Mech. / A Solids 75 (2019) 56–69.
Ustinov, K.B., R. Massabò, D. Lisovenko, Orthotropic strip with central semi-infinite crack under arbitrary loads applied far apart from the crack tip. Analytical solution. Eng. Failure Analysis 2020, 110, 104410.
Ustinov, K.B., Massabò, R., On elastic clamping boundary conditions in plate models describing detaching bilayers, Int. J. Solids Struct. (2022), in press.
Yu, H.-H., Hutchinson, J.W. 2002., Influence of substrate compliance on buckling delamination of thin films. International Journal of Fracture 113, 39-55